



## In-line quantification of micronized drug and excipients in tablets by near infrared (NIR) spectroscopy: Real time monitoring of tableting process

Atul D. Karande, Paul Wan Sia Heng, Celine Valeria Liew\*

GEA-NUS Pharmaceutical Processing Research Laboratory, Department of Pharmacy, National University of Singapore, 18 Science Drive 4, Singapore 117543, Singapore

### ARTICLE INFO

#### Article history:

Received 15 December 2009  
Received in revised form 1 June 2010  
Accepted 9 June 2010  
Available online 15 June 2010

#### Keywords:

Near infrared (NIR) spectroscopy  
Stratified sampling  
In-line sampling  
Tableting  
Content uniformity  
Continuous quality monitoring

### ABSTRACT

The objectives of this study were to assess the utility of near infrared (NIR) spectroscopy for simultaneous in-line quantification of the contents of drug and excipients in tablets and to monitor the tableting process in real time. Direct compression tablet formulations comprising micronized chlorpheniramine maleate, lactose, microcrystalline cellulose and magnesium stearate were used. A custom built NIR setup was used for in-line spectral acquisition (980–1900 nm with 1 nm resolution) during the tableting process. Calibration models using dynamic spectral acquisition were prepared and validated using design of experiment approach. During tableting, stratified sampling of tablets was also carried out to compare the NIR prediction results and subsequent UV analysis results for drug content. The results obtained with calibration and validation statistics confirmed the accuracy of models used to predict contents of tablet components. Stratified sampling results for drug content did not exhibit any significant statistical variation. However, in-line quantification enabled the content analysis of individual tablets in the production batch and detection of content uniformity problems towards the end of the tableting process. Furthermore, it provided the assurance of in-process content uniformity monitoring of the individual excipients during the tableting process.

© 2010 Elsevier B.V. All rights reserved.

### 1. Introduction

A majority of the medicaments dispensed to patients are tablet dosage forms as tablets offer many distinct advantages over other dosage forms including better drug stability, greater convenience of use and lower unit cost to manufacture. Essentially, tablets are multi-component formulations (composite matrix of drug(s) and several excipients) wherein uniform distribution of each component is critical for the desirable performance of each unit. Production batch failures, with considerable economic costs and even marketed product recalls had been the result of excessive inter-tablet dose variations. It was the well-published court decision against Barr laboratories (Berman et al., 1997) that paved the way for the introduction of stringent quality control requirements by the regulatory bodies to safeguard the public against active component variations in the final dosage. Henceforth, demonstration of content uniformity of the final powder blend as well as the finished dosage form has become a critical and mandatory validation process in solid dosage form manufacturing. However, the introduction of mandatory measures later proved to be somewhat inadequate due to certain limitations. Firstly, analysis of only 10–30 tablets from a production batch of 2–3 million tablets raises serious concerns of

having a representative sample for the whole batch. Secondly, the content uniformity assessments are generally based only on the distribution of the drug, neglecting other components (excipients) in the powder blends or tablets. Thirdly, analysis by high-performance liquid chromatography (HPLC) or ultraviolet (UV) spectroscopy is usually insensitive to the excipients; furthermore, additional analyses incur extra cost and are rarely supported by manufacturers. There is growing interest to examine alternative analytical techniques capable of analyzing drugs and excipients, and perhaps even for each and every unit dose. This development is also in line with the United States Food and Drug Administration (FDA) Process Analytical Technology (PAT) initiative and guidelines (FDA, 2004). PAT is aimed at promoting the integration of many multivariate data acquisition and analytical tools in pharmaceutical unit operations for monitoring and better understanding of critical process parameters and implementation of timely corrective action. With recent instrumentation and computing developments, the use of near infrared (NIR) spectroscopy has become a viable chemical analytical alternative as it does not require additional sample preparation and can be used for high speed real time analyses. There have been considerable literature reports on successful pharmaceutical applications of NIR spectroscopy for at-/on-/in-line analyses (Gottfried et al., 1996; Romanach and Santos, 2003; Sallam and Orr, 1985; Scheiwe et al., 1999; Thosar et al., 2001; Liew et al., 2010). Excellent reviews have also been published (Blanco and Villarroya, 2002; Luypaert et al., 2007; Roggo et al., 2007; Reich, 2005).

\* Corresponding author. Tel.: +65 65163870; fax: +65 67752265.  
E-mail address: [phalcv@nus.edu.sg](mailto:phalcv@nus.edu.sg) (C.V. Liew).

**Table 1**  
Experimental design for generation of calibration samples.

| Components        | Lower bound (% w/w) | Upper bound (% w/w) | Levels (% w/w)               |
|-------------------|---------------------|---------------------|------------------------------|
| μCPM              | 0                   | 10                  | 0, 2, 4, 6, 8, 10            |
| Lactose           | 70                  | 80                  | 70, 72, 74, 76, 78, 80       |
| MCC               | 20                  | 30                  | 20, 22, 24, 26, 28, 30       |
| MgSt <sup>a</sup> | 0                   | 1.50                | 0.50, 0.75, 1.00, 1.25, 1.50 |

<sup>a</sup> MgSt was treated as a process variable owing to its lower concentrations in tablets while generating the mixture design.

NIR spectroscopy is being extensively used in the pharmaceutical industry to determine drug content uniformity of tablets (Blanco et al., 2002; Blanco and Alcalá, 2006). However, in-/on-line quantification studies of drug in tablet dosage forms using NIR are relatively limited (Colon et al., 2005). There had been relatively less emphasis on quantification and tracking distribution of drug and excipients simultaneously in real time. Cournoyer et al. (2008) characterized tablets for multiple components but the analysis was carried out on a limited number of tablets and by a static measurement mode.

The aim of this study was to investigate the applicability of in-line NIR sensor for quantifying the contents of drug and excipients simultaneously in tablets and to monitor the tableting process in real time. The NIR spectra were obtained in the reflectance mode since this mode was reported to give results with enhanced accuracy because of the reduced sampling errors associated with moving tablets (Cogdill et al., 2005). Another growing concern for NIR non-destructive technique implementation is the likelihood of obtaining prediction results with errors almost equivalent to the traditional HPLC or UV methods. An attempt was made in this study to address this concern by developing calibration models which included maximum possible variability encountered during the actual tableting unit operation and validating these models according to International Conference on Harmonization (ICH) guidelines. Finally, in-line content uniformity analysis of drug and excipients was carried out to test the real time application of the proposed technique.

## 2. Materials and methods

### 2.1. Materials

Chlorpheniramine maleate was obtained from Merck (Singapore), Pharmatose 100M (lactose) from DMV (The Netherlands), Avicel PH102 microcrystalline cellulose (MCC) from FMC Biopolymer (USA) and magnesium stearate (MgSt) from Sigma–Aldrich (Germany). Chlorpheniramine maleate was milled in a jet mill (Hosakawa, AFG 100, Germany) at a pressure of 0.4 MPa and a classifying speed of 18,000 rpm to produce micronized chlorpheniramine (μCPM) particles with mean diameter of 3 μm. The materials were equilibrated prior to experimentation by storing for at least 48 h at 25 °C and 50% relative humidity.

### 2.2. Methods

#### 2.2.1. Calibration tablet manufacturing

A simplex lattice design was used to generate 105 calibration samples (Table 1). Calibration samples in a batch size of 100 g were prepared by mixing the respective components using a high shear mixer (Microgral, Collette NV, Belgium) followed by tumbling in a 250 mL glass bottle for 30 min. These mixing conditions were previously optimized for uniform distribution of blend components. At least 10 calibration tablets (weighing 500 mg) were compressed per 105 calibration samples using a hydraulic press (Universal Test-

ing Machine-Autograph AGE-100KN, Shimadzu, Japan) with 10 mm flat faced punches.

#### 2.2.2. Production batch tablet manufacturing

A 5 kg powder batch comprising 4% (w/w) μCPM, 72% (w/w) lactose, 23% (w/w) MCC and 1% (w/w) MgSt was mixed in an intermediate bulk container (IBC) bin blender (SP15, GEA Pharma Systems, UK) with the prism attachment for 30 min. μCPM and lactose were premixed in 10 L high shear mixer (Ultima™ Pro 10, Collette NV, Belgium) at an impeller speed 200 rpm for 3 min before proceeding to mix with MCC and MgSt in the IBC. The mixed blend was then emptied into a 10 L hopper for tablet compression in a 10 station rotary tableting machine (Rimek, India) using 10 mm flat faced punches. The machine was operated at a speed of 10 rpm. The average tablet weight was 530 mg.

#### 2.2.3. Calibration and production (in-line) NIR spectral acquisition

NIR spectral sensor (MCS 611 NIR 2.2, Carl Zeiss, Germany) and NIR diffuse reflectance measurement probe (QR600-7, Ocean Optics, USA) with a 3.18 mm diameter spot size were used to obtain the NIR spectra of the calibration and production batch tablets. The setup used allowed spectral acquisition of 980–1900 nm with 1 nm resolution.

The setup used for spectral acquisition of tablets is shown in Fig. 1. The fibre optic probe was positioned inside the metallic holder and mounted on the tableting machine just adjacent to the tablet ejection area. A clearance of 0.5 mm between the tablet and probe was always maintained to avoid errors associated with the sampling distance.

For calibration tablets, the punches and dies were removed and dies were replaced with the blank discs. The tablets were lined up near the tablet ejection area and the turret was rotated at 10 rpm. The NIR sensor was triggered while the tablets were passing underneath the measuring head of the probe. Reflection spectra were acquired through the fibre optic probe and processed on a computer using the Aspect Plus (version 1.76, Carl Zeiss, Germany) and Process Explorer (version 1.1.0.6, Carl Zeiss, Germany) softwares. For in-line spectral acquisition during tableting, a similar procedure was used with the punches and dies fixed. In order to exclude non-sample data (when NIR sensor was not triggered on the tablet surface), a trend qualification rule was set in the Process Explorer method setup which removed the non-representative spectra from the data stream.

#### 2.2.4. Calibration model development

Unscrambler 9.8 (version 9.8, Camo Inc., India) was used off-line to build the calibration models. The raw calibration spectra were preprocessed using standard normal variate (SNV) followed by derivative preprocessing. All first and second derivative spectra were computed employing 9 smoothing points and 2nd polynomial order. Partial least square (PLS1) regression technique was used to build the calibration models except for the signature wavelengths models for which multi-linear regression (MLR) technique was used. The reference values used for calibration samples were calculated gravimetrically from the actual weights of the calibration mixtures (% ingredient A = 100 × weight of ingredient A/total weight of tablet).

Several sets of calibration models were developed using different spectral regions (980–1400, 1400–1900 and 980–1900 nm) and signature wavelengths for each components (μCPM–1124, lactose–1538, MCC–1489, MgSt–1408 nm) to find the best calibration model. Additional models were also built using the significant wavelengths obtained after Martens' jack-knife significance test (Westad et al., 1999; Esbensen, 2004; Marten and Naes, 1989) was performed on whole wavelength spectral data. In this

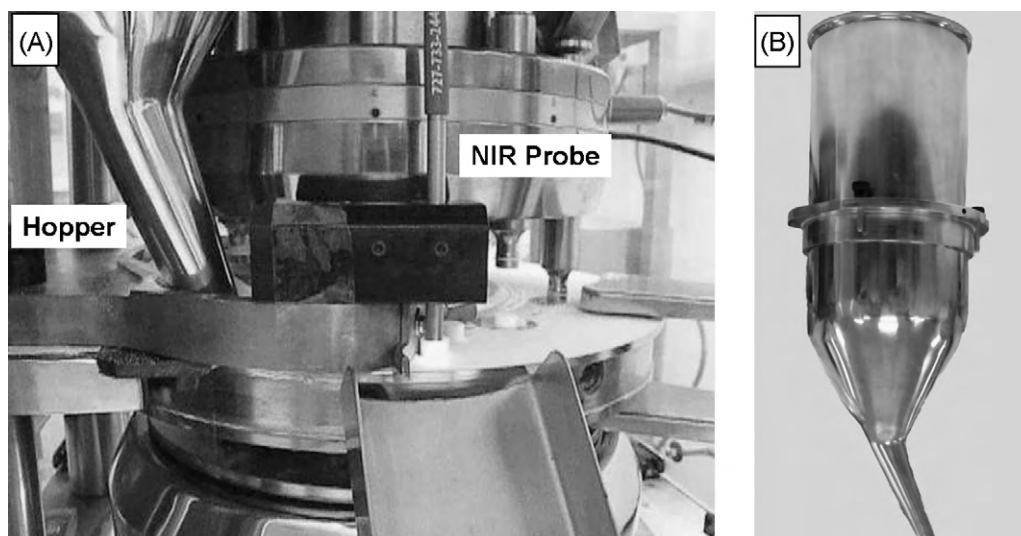


**Fig. 1.** Experimental setup for the in-line quantification of drug and excipients during tableting. (A) Rotary tablet press with NIR probe and (B) Hopper.

test, under cross validation, a number of sub-models were created which were based on all the calibration samples that were not kept out in the cross validation segment. For every sub-model, regression coefficients were calculated. For each wavelength, the difference between the regression coefficient in a sub-model and the regression coefficient for the total model (model based on all the samples) was calculated. The sum of the squares of the differences in all sub-models was calculated to obtain an expression of the variance of the estimate of regression coefficient in a sub-model for a wavelength. A *t*-test was then applied to determine the significance of the estimate of regression coefficient in a sub-model. Resultant regression coefficients with uncertainty limits that corresponded to 2 standard deviations and/or those which did not cross the zero line were considered as significant variables. More detailed description of this test could be found in the reference (Esbensen, 2005).

#### 2.2.5. Validation of calibration models

Leave one out full cross validation was carried out for all the calibration models. Additionally, external test set validation and validation according to ICH guidelines were carried out for the selected optimal models. For external test validation, at least 10 tablets (weighing 500 mg) per 34 independent validation tablets falling within the range of calibration tablets were prepared using the hydraulic press and scanned using a procedure similar to that used for generating the calibration tablets. The spectra obtained from 10 tablets per validation tablet were averaged and used for further processing. Respective test set validation models for each component were then constructed and tested based on the figures of merits.

The validated calibration models for each component were then uploaded into the Process Explorer using the Online Unscrambler Predictor (OLUP) software for in-line quantification of components. OLUP packaged calibration models into a dynamic link library (DLL, 32 bit only) protocol. Through these protocols, Process Explorer was interfaced with the OLUP for in-line quantification of each component.

#### 2.2.6. Content uniformity of production tablets obtained using stratified sampling

During production batch tableting, tablets were collected immediately after in-line spectral acquisition into three separate containers. The containers were changed at every 30 min interval.

At the end of the tablet production process, 30 tablets from each container were randomly withdrawn and weighed before performing further analysis. These tablets were then scanned in a dynamic manner using the same procedure as that for the calibration tablets. A laboratory validated UV spectroscopic method was used to determine the drug content uniformity of each batch of tablets. Each individual tablet was weighed in a volumetric flask and diluted to 200 ml with distilled water. The flask was then shaken and ultrasonicated for 10 min to ensure complete disintegration of the tablet. Approximately 20 mL aliquot per sample was subjected to centrifugation at 2000 rpm for 5 min and the resultant supernatant solution was analyzed for the concentration of  $\mu$ CPM using a UV spectrophotometer (UV-3101 PC, Shimadzu, Japan) at 262 nm.

### 3. Results and discussion

#### 3.1. Effective surface area sampled by NIR probe

Effective tablet surface area sampled by NIR probe was determined based on the distance travelled by the moving tablet under the illuminated spot of 3.18 mm diameter of the NIR probe. Considering the experimental conditions used, it was estimated that the 3.18 mm spot would traverse a distance of 1.66 mm during its scanning across the tablet surface. Thus, the effective surface area, i.e. area sampled by NIR probe, was 13.221 mm<sup>2</sup>. There was an added advantage of employing dynamic sampling (moving tablets) as it actually enabled the scanning of a larger tablet surface than a stationary illuminated spot measurement of 3.18 mm diameter. Furthermore, with the usage of this dimension, it was possible to determine the occurrence of non-uniform distribution resulting from the agglomeration of very fine  $\mu$ CPM particles (3  $\mu$ m) which would not have been feasible with analysis of the whole area of the tablet surface. In a recent investigation, Li et al. (2003) demonstrated that spectral analysis of a small part of the tablet is an acceptable replacement for whole tablet analysis using traditional HPLC/UV.

#### 3.2. Effect of sampling strategies on NIR spectra

Preliminary experiments were carried out to examine the effect of sampling strategies on the NIR spectral features of the tablets. Target formulation tablets compressed using rotary press were subjected to NIR spectral acquisition using static and dynamic

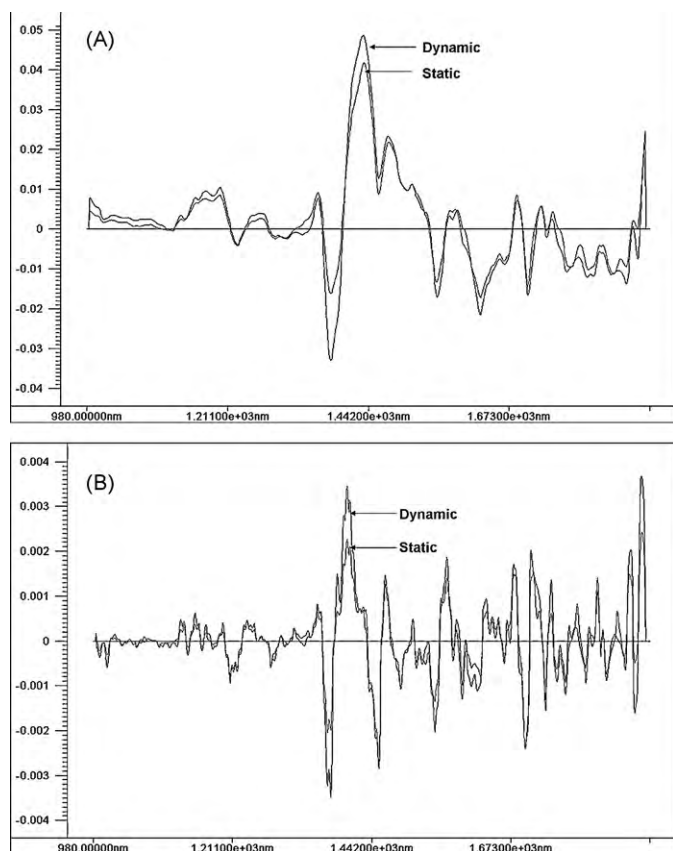


**Fig. 2.** Spectral differences observed for the same tablet with dynamic and static sampling strategies. (A) SNV followed by 1st derivative spectra and (B) SNV followed by 2nd derivative spectra. In these plots, X and Y axes represent the wavelength (nm) and absorbance, respectively.

strategies. The obtained spectra were pretreated with SNV followed by 1st derivative, and SNV followed by 2nd derivative preprocessing. Careful examination of the spectra (Fig. 2) obtained using different strategies showed the exhibition of distinct spectral differences. The observed spectral differences illustrated the importance of adopting appropriate and similar sampling strategies for both calibration and actual testing, i.e. real time tableting process. Hence, it was decided to capture the NIR spectra of the cal-

ibration tablets in a dynamic mode so as to simulate the movement of tablets during real time tableting process.

### 3.3. Calibration model development

In NIR spectroscopy, spectral preprocessing and spectral regions to be used for building the calibration models are of crucial importance. Spectral preprocessing is usually performed to remove unwanted scattering features incorporated in NIR spectra which are often due to the differences in sizes of the constituent particles and other interfering factors which do not provide any information about the chemical concentration of the analyte of interest (Blanco et al., 1997; Olinger and Griffiths, 1993a,b). On the other hand, it is a general principle that a parsimonious model, i.e. a model with fewer components and variables than the full components or variables, will result in a model with optimal calibration statistics since the number of model parameters is sparse. However, it could be advantageous in some cases to keep some of the wavelengths (X) with even the slightest correlation (with respect to the component (Y)) to span the multi-dimensional space especially when the sample is moving, or varies rapidly with time (Honigs, 1992; Beebe et al., 1998; Esbensen, 2005). As can be seen from Fig. 3, all the tablet components exhibited regions of meaningful correlations throughout the range but almost all the regions were overlapping. Thus, different strategies were used to determine the appropriate spectral preprocessing and spectral regions for obtaining the optimal calibration models. Performances of the models were compared on the basis of figures of merits as shown in Tables 2 and 3.

All the models built using respective signature wavelengths for each of the blend components showed inferior performance in terms of figures of merits, irrespective of the spectral preprocessing technique employed. This is quite interesting as most previous studies based on static spectral acquisition reported improved performances of models after restricting the wavelengths to where the specific regions were. In static acquisition, occurrence of spectral shifts is unlikely as the calibration sample/tablet surface is always stationary under the probe during measurement as compared to dynamic acquisition where the calibration sample is subjected to continuous movement during measurement. Hence, inferior performances of models built using signature wavelengths could be attributed to the spectral shift.

In the case of PLS1 models built using different wavelength ranges, the performances of calibration models were found to be

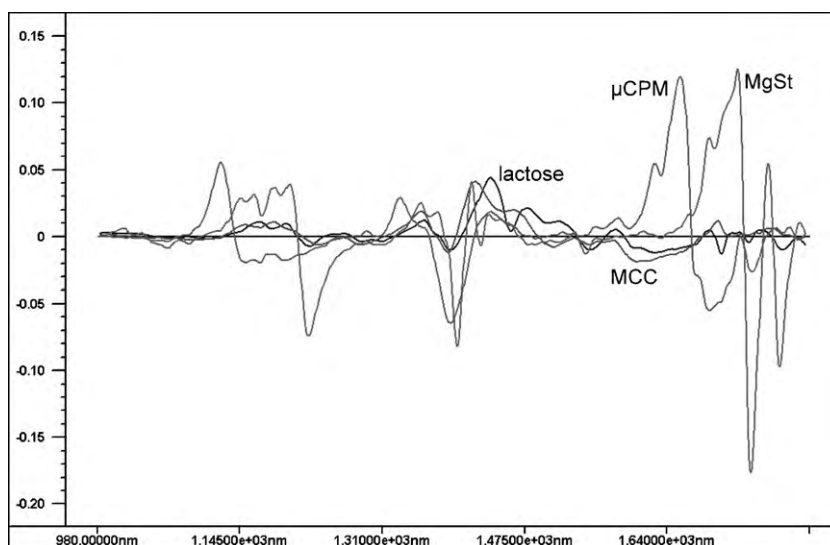


**Fig. 3.** SNV followed by 1st derivative preprocessed NIR reflectance spectra of tablet components in powder form. In this plot, X and Y axes represent the wavelength and absorbance, respectively.

**Table 2**

Summary of the figures of merits obtained for calibration models based on SNV followed by 1st derivative pretreated spectra.

| Components                   | No. of PC | Explained variance (%) |       | Calibration    |           |            |
|------------------------------|-----------|------------------------|-------|----------------|-----------|------------|
|                              |           | X                      | Y     | R <sup>2</sup> | RMSEC (%) | RMSECV (%) |
| Spectral region 980–1900 nm  |           |                        |       |                |           |            |
| μ.CPM                        | 4         | 90.00                  | 94.92 | 0.961          | 0.572     | 0.603      |
| Lactose                      | 6         | 90.27                  | 90.66 | 0.942          | 0.696     | 0.797      |
| MCC                          | 6         | 91.12                  | 88.22 | 0.927          | 0.797     | 0.904      |
| MgSt                         | 4         | 91.08                  | 94.12 | 0.947          | 0.080     | 0.084      |
| Martens' jack-knifing        |           |                        |       |                |           |            |
| μ.CPM                        | 4         | 90.62                  | 94.90 | 0.952          | 0.585     | 0.604      |
| Lactose                      | 6         | 91.25                  | 90.06 | 0.914          | 0.847     | 0.909      |
| MCC                          | 6         | 91.15                  | 87.50 | 0.915          | 0.863     | 0.958      |
| MgSt                         | 4         | 90.61                  | 84.02 | 0.845          | 0.137     | 0.139      |
| Spectral region 980–1400 nm  |           |                        |       |                |           |            |
| μ.CPM                        | 9         | 90.15                  | 90.94 | 0.937          | 0.669     | 0.676      |
| Lactose                      | 5         | 90.00                  | 75.32 | 0.831          | 1.211     | 1.322      |
| MCC                          | 5         | 93.75                  | 71.63 | 0.853          | 1.138     | 1.289      |
| MgSt                         | 5         | 90.96                  | 84.22 | 0.868          | 0.126     | 0.131      |
| Spectral region 1400–1900 nm |           |                        |       |                |           |            |
| μ.CPM                        | 5         | 90.01                  | 92.75 | 0.934          | 0.675     | 0.711      |
| Lactose                      | 6         | 90.74                  | 84.01 | 0.864          | 1.064     | 1.157      |
| MCC                          | 5         | 90.59                  | 79.64 | 0.880          | 1.036     | 1.188      |
| MgSt                         | 5         | 91.85                  | 91.92 | 0.939          | 0.085     | 0.089      |
| Signature wavelengths (MLR)  |           |                        |       |                |           |            |
| μ.CPM                        | –         | –                      | –     | 0.871          | 0.919     | 0.923      |
| Lactose                      | –         | –                      | –     | 0.615          | 1.629     | 1.636      |
| MCC                          | –         | –                      | –     | 0.740          | 1.538     | 1.551      |
| MgSt                         | –         | –                      | –     | 0.867          | 0.128     | 0.129      |

PC represents principal components, R<sup>2</sup>: correlation coefficient, RMSEC: root mean square error of calibration; RMSECV: root mean square error of prediction obtained with *leave one out full cross validation*. Martens' jack-knifing indicates the PLS1 calibration models built using significant wavelengths suggested by Martens' jack-knife significance test.

better when SNV followed by 1st derivative spectra was used. Y explained variances for all the models reduced, particularly when they were built using SNV followed by 2nd derivative spectra. However, models built using significant wavelengths obtained after Martens' jack-knife significance test resulted in somewhat similar

performances compared to those built using full wavelength range. The largest RMSEC (root mean square error of calibration) and RMSECV (root mean square error of prediction obtained with *leave one out full cross validation*) were observed for the low wavelength region (980–1400 nm). Moreover, X and Y explained variances

**Table 3**

Summary of the figures of merits obtained for calibration models based on SNV followed by 2nd derivative pretreated spectra.

| Components                   | No. of PC | Explained variance (%) |       | Calibration    |           |            |
|------------------------------|-----------|------------------------|-------|----------------|-----------|------------|
|                              |           | X                      | Y     | R <sup>2</sup> | RMSEC (%) | RMSECV (%) |
| Spectral region 980–1900 nm  |           |                        |       |                |           |            |
| μ.CPM                        | 6         | 69.85                  | 89.53 | 0.916          | 0.867     | 0.969      |
| Lactose                      | 8         | 69.71                  | 85.74 | 0.911          | 0.845     | 1.074      |
| MCC                          | 8         | 68.95                  | 76.84 | 0.829          | 1.179     | 1.374      |
| MgSt                         | 6         | 68.97                  | 91.77 | 0.930          | 0.090     | 0.098      |
| Martens' jack-knifing        |           |                        |       |                |           |            |
| μ.CPM                        | 4         | 62.65                  | 91.86 | 0.924          | 0.817     | 0.847      |
| Lactose                      | 8         | 68.37                  | 79.99 | 0.843          | 1.146     | 1.292      |
| MCC                          | 7         | 70.77                  | 78.16 | 0.821          | 1.205     | 1.335      |
| MgSt                         | 5         | 71.53                  | 91.50 | 0.922          | 0.096     | 0.099      |
| Spectral region 980–1400 nm  |           |                        |       |                |           |            |
| μ.CPM                        | 5         | 72.90                  | 93.18 | 0.937          | 0.720     | 0.750      |
| Lactose                      | 7         | 74.01                  | 82.73 | 0.856          | 1.130     | 1.239      |
| MCC                          | 7         | 71.83                  | 79.73 | 0.836          | 1.191     | 1.326      |
| MgSt                         | 7         | 75.33                  | 84.61 | 0.864          | 0.127     | 0.135      |
| Spectral region 1400–1900 nm |           |                        |       |                |           |            |
| μ.CPM                        | 5         | 68.24                  | 88.84 | 0.900          | 0.877     | 0.928      |
| Lactose                      | 8         | 68.85                  | 82.91 | 0.874          | 1.006     | 1.176      |
| MCC                          | 7         | 67.18                  | 82.62 | 0.868          | 1.055     | 1.211      |
| MgSt                         | 6         | 68.90                  | 91.42 | 0.927          | 0.093     | 0.101      |
| Signature wavelengths (MLR)  |           |                        |       |                |           |            |
| μ.CPM                        | –         | –                      | –     | 0.827          | 1.275     | 1.283      |
| Lactose                      | –         | –                      | –     | 0.808          | 1.334     | 1.342      |
| MCC                          | –         | –                      | –     | 0.798          | 1.352     | 1.360      |
| MgSt                         | –         | –                      | –     | 0.734          | 0.158     | 0.159      |

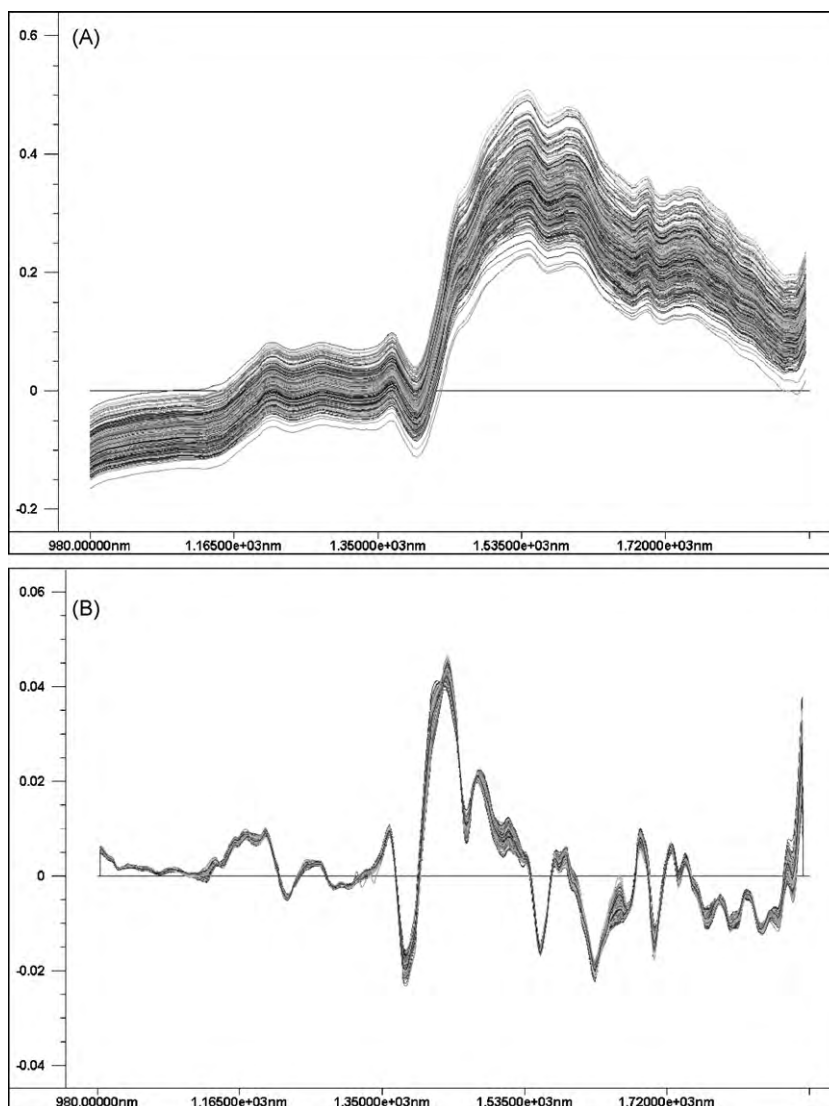


**Fig. 4.** NIR reflectance spectra of calibration batch tablets. (A) Raw and (B) SNV followed by 1st derivative preprocessed. In these plots, X and Y axes represent the wavelength and absorbance, respectively.

with models developed using narrow ranges (both 980–1400 and 1400–1900 nm) were inferior compared to those using entire wavelength range. Fig. 4A and B shows the raw and SNV followed by 1st derivative preprocessed spectra of calibration tablets for the entire spectral range of 980–1900 nm. Fig. 4B depicts the correction of both shift and curvature of the baseline obtained after processing the spectra with SNV followed by first derivative.

The improved performance with the entire wavelength range models could be attributed to the incorporation of multivariate data averaging effect where regions/wavelengths even with the slightest correlation were also utilized for model development (Beebe et al., 1998). Previous studies have shown the improved performance of calibration models after narrowing down the wavelength range (El-Hagrasy and Drennen, 2006). However, for the present study, an opposite trend was observed, possibly due to the wider spread of the high correlation regions/wavelengths of the analytes (tablet components). These results concur with the findings reported by Meza et al. (2006) where they attributed the improved performance of the calibration model to the inclusion of many wavelengths with slightest correlation while building the calibration models. Based on this finding, the calibration model for each component included the entire spectral range, i.e. 980–1900 nm, pretreated with SNV followed by 1st derivative spectral preprocessing.

Among the models involving the entire spectral range, the  $\mu$ CPM and MgSt models showed excellent results in terms of explained variances and residual errors at the calibration and validation stages. This could be attributed to the action of dry powder coating of the coarse excipients by the numerically larger, fine  $\mu$ CPM and MgSt particles during mixing of the blend components. Thus, the measuring head encountered the  $\mu$ CPM and MgSt boundaries at a much higher frequency than those of the coarser lactose and MCC.

#### 3.4. Validation according to ICH guidelines

As the calibration models were developed based on dynamic spectral data, it was imperative to test the adequacy and applicability of the model for process analysis. The proposed NIR method was validated in accordance with the ICH guidelines for accuracy, repeatability, intermediate precision and linearity (ICH, 2005).

##### 3.4.1. Linearity

The linearity of an analytical method can be defined as its ability, within a given range, to predict the concentration of test (unknown) samples which are directly proportional to the concentration of analyte in the (known) samples. Linearity was confirmed on the basis of the  $R^2$  values of regression lines obtained from the plots of

**Table 4**Validation results obtained with the *leave one out full cross validation* and test set validation.

| Statistics          | $\mu$ CPM |        | Lactose |       | MCC    |       | MgSt  |       |
|---------------------|-----------|--------|---------|-------|--------|-------|-------|-------|
|                     | FCV       | TSV    | FCV     | TSV   | FCV    | TSV   | FCV   | TSV   |
| Samples             | 105       | 34     | 105     | 34    | 105    | 34    | 105   | 34    |
| Slope               | 0.949     | 0.871  | 0.927   | 0.890 | 0.904  | 0.922 | 0.939 | 0.794 |
| Offset              | 0.144     | 0.247  | 5.292   | 8.188 | 2.230  | 2.181 | 0.059 | 0.205 |
| Correlation         | 0.974     | 0.970  | 0.961   | 0.944 | 0.951  | 0.949 | 0.970 | 0.975 |
| $R^2$               | 0.949     | 0.944  | 0.924   | 0.887 | 0.906  | 0.903 | 0.941 | 0.926 |
| RMSECV(%)           | 0.603     | –      | 0.797   | –     | 0.904  | –     | 0.084 | –     |
| RMSE (%)            | –         | 0.869  | –       | 0.844 | –      | 0.800 | –     | 0.097 |
| Bias                | –0.001    | –2.891 | –0.001  | 0.214 | –0.001 | 0.458 | 0.000 | 0.013 |
| SD of residuals (%) | –         | 0.453  | –       | 0.902 | –      | 0.785 | –     | 0.081 |

FCV: *leave one out full cross validation* statistics, TSV: test set validation statistics, RMSE: root mean square error of prediction with test set, SD of residuals: standard deviation of residuals after test set validation.

NIR model predicted values and reference values at the calibration and test set validation stages. All the models were found to exhibit linearity within the span of calibration and validation range as confirmed from the  $R^2$  values (Table 4). Fig. 5 depicts the predicted vs. measured plot for each tablet component.

### 3.4.2. Accuracy

Accuracy of the models developed was estimated based on RMSECV and bias values obtained from the *leave one out full cross validation* and on RMSE (root mean square error of prediction with test set) and bias values obtained from the test set validation. Results obtained for RMSECV, RMSE and bias values confirmed the accuracy of the models for predicting the concentration of tablet components. A further estimate of accuracy for each component was given by the standard deviation of the residuals obtained after the test set validation (Table 4).

### 3.4.3. Repeatability

Repeatability, an indicator of precision under the same conditions over a short interval of time, was assessed according to the ICH specifications which require: (a) a minimum of 6 readings of a single sample at 100% target concentration, and (b) a minimum of 3 samples, one at each of the 3 levels of concentration. Tablets with  $\mu$ CPM concentration at 3 levels were used. Each tablet was scanned and 10 spectra were obtained per tablet and the concentration of each component was predicted using respective calibration models. % RSD (relative standard deviation) values of lower than 2 were obtained for all the tablet components (Table 5) indicating that there was adequate exhibition of repeatability of predictions by the models applied.

### 3.4.4. Intermediate precision

Intermediate precision, an indicator of precision under the influence of random events during the analysis, was determined by

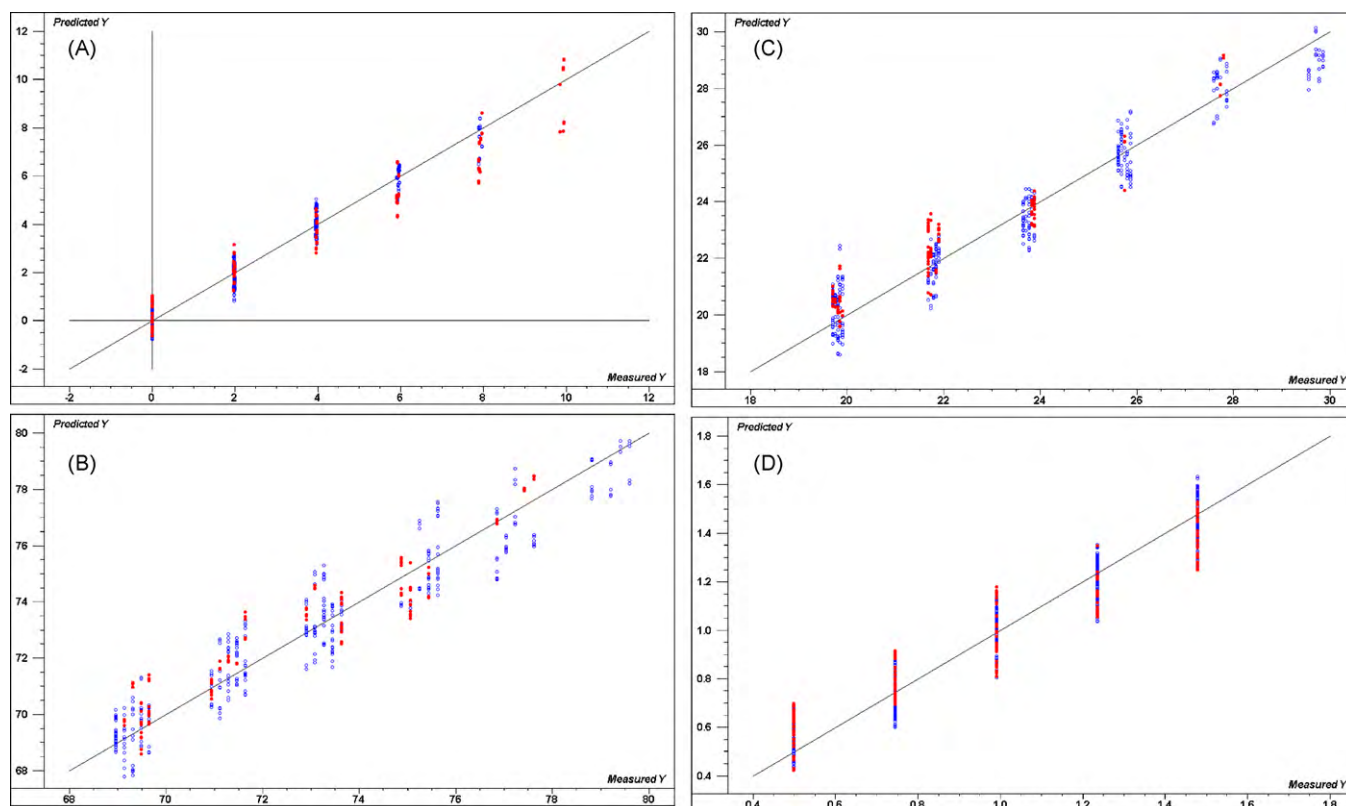


**Fig. 5.** PLS regression models for (A)  $\mu$ CPM, (B) lactose, (C) MCC and (D) MgSt. Points in blue colour in the regression plots indicate the calibration samples ( $n = 105$ ) and those in red colour are test set validation samples ( $n = 34$ ). (For interpretation of the references to color in this figure legend, the reader is referred to the web version of the article.)

**Table 5**  
Results of repeatability and intermediate precision.

| Statistics             | Tablet 1  |         |       |       | Tablet 2  |         |       |       | Tablet 3  |         |       |       |
|------------------------|-----------|---------|-------|-------|-----------|---------|-------|-------|-----------|---------|-------|-------|
|                        | $\mu$ CPM | Lactose | MCC   | MgSt  | $\mu$ CPM | Lactose | MCC   | MgSt  | $\mu$ CPM | Lactose | MCC   | MgSt  |
| Repeatability          |           |         |       |       |           |         |       |       |           |         |       |       |
| Mean (% w/w)           | 2.55      | 70.73   | 27.45 | 1.11  | 4.40      | 69.86   | 28.19 | 1.10  | 6.13      | 69.24   | 31.98 | 0.96  |
| % RSD                  | 0.96      | 0.30    | 0.91  | 1.39  | 0.59      | 0.33    | 0.68  | 1.19  | 0.63      | 0.24    | 0.77  | 1.96  |
| Intermediate precision |           |         |       |       |           |         |       |       |           |         |       |       |
| Inter-day              |           |         |       |       |           |         |       |       |           |         |       |       |
| <i>p</i> value         | 0.37      | 0.60    | 0.49  | 0.93  | 0.70      | 0.37    | 0.85  | 0.51  | 0.83      | 0.64    | 0.44  | 0.81  |
| <i>F</i> experiment    | 1.70      | 0.67    | 0.15  | 0.08  | 0.44      | 1.68    | 0.18  | 0.95  | 0.21      | 0.58    | 1.28  | 0.24  |
| <i>F</i> critical      | 19.00     | 19.00   | 19.00 | 19.00 | 19.00     | 19.00   | 19.00 | 19.00 | 19.00     | 19.00   | 19.00 | 19.00 |
| Inter-analyst          |           |         |       |       |           |         |       |       |           |         |       |       |
| <i>p</i> value         | 0.37      | 0.60    | 0.49  | 0.29  | 0.37      | 0.64    | 0.29  | 0.20  | 0.97      | 0.11    | 0.25  | 0.88  |
| <i>F</i> experiment    | 4.12      | 2.57    | 0.70  | 2.04  | 1.32      | 0.30    | 2.09  | 3.67  | 0.00      | 7.80    | 2.60  | 0.03  |
| <i>F</i> critical      | 18.51     | 18.51   | 18.51 | 18.51 | 18.51     | 18.51   | 18.51 | 18.51 | 18.51     | 18.51   | 18.51 | 18.51 |

analyzing tablets for  $\mu$ CPM concentration at 3 levels on two different days and by two analysts, each carrying out the analysis on a different day. Results of the intermediate precision studies are as shown in Table 5. Two-factor analysis of variance (ANOVA) was performed on the data and it did not show any statistically significant differences between analysts and days for tablet testing.

### 3.5. Application of developed models for real time tableting process analysis

#### 3.5.1. System performance for real time application

Results obtained from the initial calibration and validation studies confirmed the accuracy of the developed NIR models to predict the concentration of the tablet components. However, the next objective was to apply the developed models for their application in real time monitoring during the tableting process. Considering the differences between the tablets prepared at the calibration stage by a hydraulic press and production stage by a rotary press, the occurrence of spectral artefacts was anticipated. These artefacts could be detrimental to cross correlation studies and may lead to erroneous predictions. Hence, it was imperative to standardize the measured spectra in order to minimize the incorporation of process borne effects during predictions. A possible treatment to minimize such differences was to standardize the spectral acquisition times during the calibration and production stages and to pretreat the spectra with suitable preprocessing techniques which had been shown to be able to minimize such effects. A fixed integration time of 100 ms for spectral acquisition and different pretreatments were adopted at the calibration and production stages of analyses. Batches of tablets with  $\mu$ CPM concentration at 6 levels (0%, w/w; 2%, w/w; 4%, w/w; 6%, w/w; 8%, w/w and 10%, w/w) were prepared independently using the hydraulic press and rotary press. After compression using the hydraulic press, the NIR spectra of tablets were obtained according to the procedure described for calibration tablets. Rotary press tablets were scanned in-line during tableting. Efficiency of the conditions was tested by analyzing the spectra using principal component analysis (PCA) and by comparing predictions of content of individual formulation components using the respective models (Fig. 6). For PCA, the spectra were normalised using 1/standard deviation scaling so as to bring the score to equal scales. Among the different pretreatments used, SNV followed by 1st derivative showed excellent results in terms of reducing the effects arising from differences in the compression process employed as evident from the reduced scattering within the scores plots. The distance between the scores of the tablets of same formulation but compressed using hydraulic and rotary process was found to be reduced in the scores plot obtained from preprocessed spectra. Furthermore, the predictions results

(Table 6) obtained for content of each tablet component revealed no statistically significant differences between tablets compressed using the hydraulic press and rotary press (*p* value > 0.05 obtained with a paired *t* test at 95% confidence interval).

#### 3.5.2. In-line analysis of tablets

In-line quantification of the formulation components during tableting was carried out using the setup described in the experimental section. The turret of the tableting machine was rotated at 10 rpm which ultimately resulted in the production rate of  $100 \pm 3$  tablets/min. Considering the tableting speed, an integration time of 100 ms was adequate for scanning a sufficient area of one tablet at each trigger. In-line spectral acquisition was carried out over 100 min. Thus, approximately 10,000 tablets were scanned during the acquisition process. The spectral data was divided into three periods of the tableting operation, i.e. 0–30, 30–60 and 60–100 min, in order to determine any deviation in content uniformity during the tableting process. Frequency distribution plots (Fig. 7) for  $\mu$ CPM per period were constructed from the individual prediction values obtained.

One of the major limitations for the analysis of the data in the present study was the non-existence of scale of scrutiny guidelines for excipients unlike for the active component in the formulation. For ease of analysis, only the active, i.e.  $\mu$ CPM, was subjected to the USP specified scale of scrutiny. However, it was recognized that a casual check of concentration values would also be useful to mark the occurrence of non-uniform distribution of excipients within the powder blend in the hopper during the tableting process.

Mean  $\mu$ CPM concentration of the tablets and % RSD values for each component obtained from in-line predictions are depicted in Tables 7 and 8. The highest and lowest concentrations of  $\mu$ CPM were 114.63% and 85.06% during the first 30 min. These results passed the USP criteria (2009) of  $100 \pm 15\%$  content and % RSD of not more than 6%, confirming that the drug particles were uniformly distributed in the tablets. However, deviation in content uniformity was observed midway through the tableting process and deteriorated towards the end stage as can be seen from the skewed frequency distribution plots for  $\mu$ CPM (Fig. 7(A-2 and A-3)).

The results of this in-line NIR study revealed the occurrence of segregation towards the end of the tableting process as shown by reductions in mean concentrations of both  $\mu$ CMP and lactose and a slight increase in concentration of MCC (Tables 7 and 8). This occurrence of segregation in an initially well-blended 5 kg powder as used in the present study (even in the absence of an unusual high vibration frequency) was due to the considerable disparities in the physical characteristics of the blend components, i.e. size and density, and the hopper geometry (bin hopper with a tapered end (Fig. 1(B))).



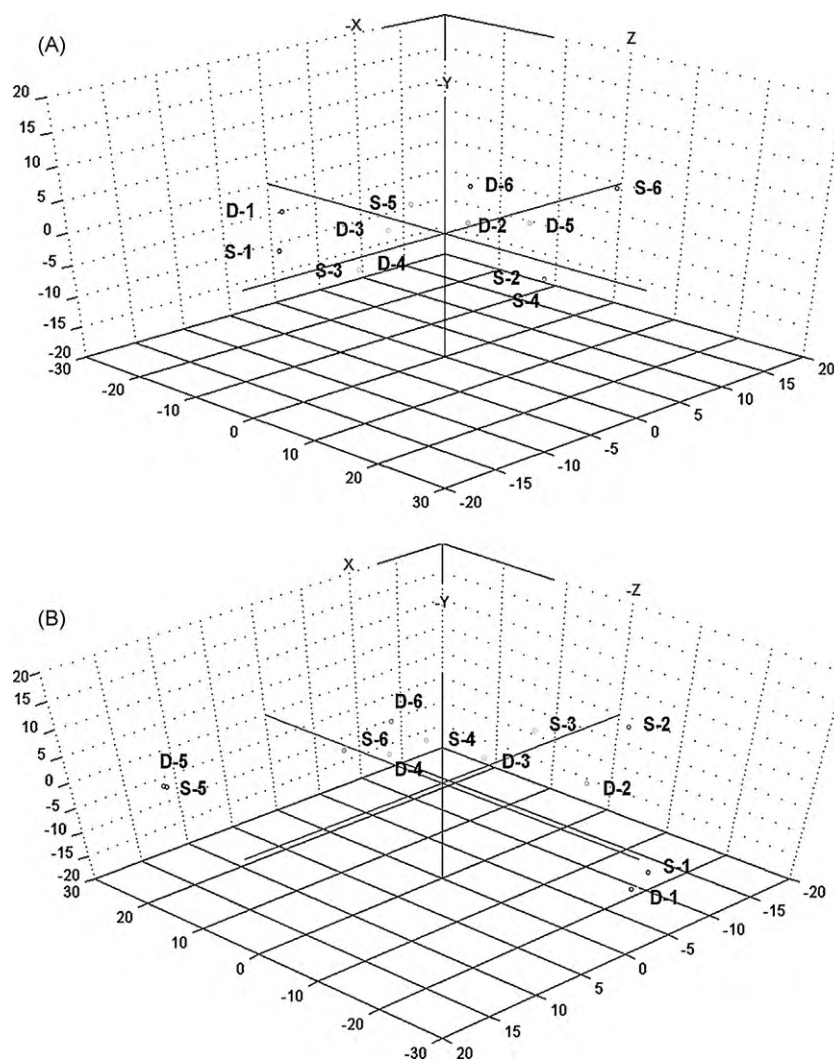


**Fig. 6.** Scores plot for the spectra obtained after PCA. (A) Raw spectra and (B) spectra treated with SNV followed by 1st derivative. S-*n* represents the tablets compressed using hydraulic press and D-*n* represents the tablets compressed using rotary press.

A non-skewed content uniformity histogram was obtained for the tablets compressed during the initial 0–30 min period as depicted in Fig. 7(A-1). During their residence in the hopper, the lactose particles coated with fine  $\mu$ CMP particles (Fig. 8) behaved as individual ordered units as they had been premixed using a high shear mixer before mixing with the remaining excipients in an IBC. Initially, the powder blend underwent mass flow pattern on a first in/first out basis. This particu-

lar flow pattern exhibited by the blend promoted uniform flow of the blend components for tableting. As more and more of the blend was utilized (30–60 min), a skewed distribution of the content uniformity data was obtained (Fig. 7(A-2)). This was attributed to the slight change in flow pattern which caused a greater degree of channelling at the core region of the powder bed and development of a shallow v-shaped powder surface.

**Table 6**  
Effect of compression process on the prediction results obtained from NIR models.

| Tablet formulation | Tablet component (% w/w) |        |           |         |        |           |        |        |           |       |        |           |
|--------------------|--------------------------|--------|-----------|---------|--------|-----------|--------|--------|-----------|-------|--------|-----------|
|                    | $\mu$ CMP                |        |           | Lactose |        |           | MCC    |        |           | MgSt  |        |           |
|                    | Ref                      | Rotary | Hydraulic | Ref     | Rotary | Hydraulic | Ref    | Rotary | Hydraulic | Ref   | Rotary | Hydraulic |
| 1                  | 0.000                    | -0.408 | -0.019    | 69.301  | 73.010 | 72.044    | 29.703 | 30.982 | 32.086    | 0.990 | 1.140  | 0.990     |
| 2                  | 1.980                    | 1.919  | 1.967     | 77.222  | 78.688 | 76.355    | 19.802 | 19.763 | 21.743    | 0.990 | 0.982  | 0.968     |
| 3                  | 3.960                    | 4.302  | 4.822     | 73.267  | 73.475 | 74.048    | 21.782 | 22.104 | 22.869    | 0.990 | 1.007  | 0.894     |
| 4                  | 5.941                    | 6.632  | 6.408     | 71.287  | 70.802 | 69.720    | 21.782 | 22.516 | 20.132    | 0.990 | 0.921  | 0.937     |
| 5                  | 7.921                    | 8.029  | 8.254     | 71.287  | 71.909 | 72.414    | 19.802 | 18.281 | 16.864    | 0.990 | 1.192  | 0.901     |
| 6                  | 9.901                    | 11.503 | 11.486    | 69.301  | 66.346 | 63.861    | 19.802 | 18.075 | 21.979    | 0.990 | 1.112  | 1.052     |
| Mean               |                          | 5.330  | 5.486     |         | 72.372 | 71.407    |        | 21.954 | 22.612    |       | 1.059  | 0.957     |
| <i>p</i> value     |                          | 0.221  |           |         | 0.134  |           |        | 0.511  |           |       | 0.074  |           |

"Ref" indicates gravimetric reference values of the tablet components, "Rotary" and "Hydraulic" indicate the NIR predicted values of components of tablets compressed using rotary and hydraulic press.

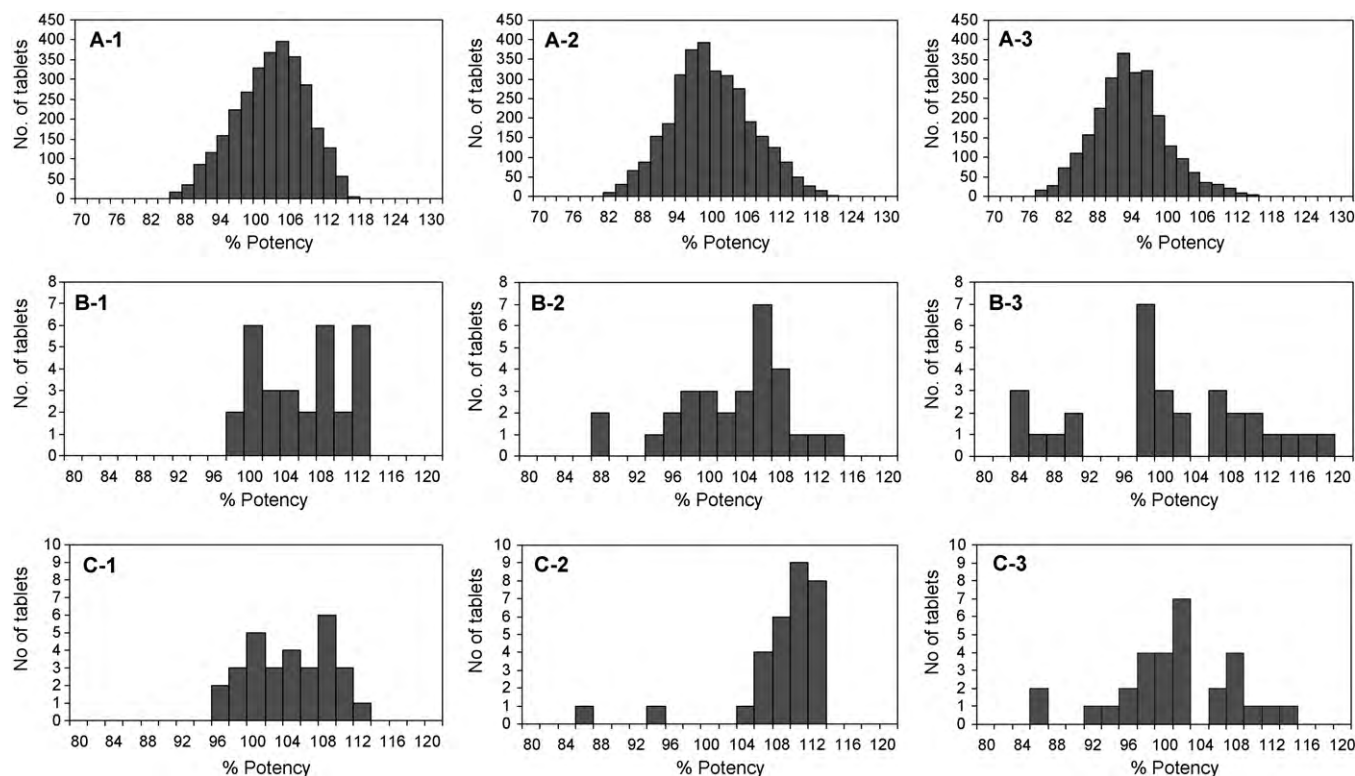


**Fig. 7.** Frequency distribution plots of individual tablet potency in terms of  $\mu$ CPM obtained from (A-1 to A-3) in-line NIR, (B-1 to B-3) stratified NIR and (C-1 to C-3) stratified UV analysis. The numbers 1, 2 and 3 indicate the time periods of 0–30, 30–60 and 60–100 min during tableting.

**Table 7**  
Comparison of  $\mu$ CPM (% potency) in-line NIR predictions, stratified NIR predictions and stratified UV analysis results.

| Mode                     | In-line NIR |        |        | Stratified NIR |        |        | Stratified UV |        |        |
|--------------------------|-------------|--------|--------|----------------|--------|--------|---------------|--------|--------|
|                          | 0–30        | 30–60  | 60–100 | 0–30           | 30–60  | 60–100 | 0–30          | 30–60  | 60–100 |
| Minimum                  | 85.06       | 80.18  | 76.23  | 97.55          | 87.23  | 84.38  | 95.39         | 85.33  | 85.23  |
| Maximum                  | 114.63      | 118.94 | 127.84 | 111.78         | 112.80 | 112.73 | 110.55        | 111.85 | 113.81 |
| OOS tablets <sup>a</sup> | 0           | 86     | 302    | 0              | 0      | 1      | 0             | 0      | 0      |
| Mean                     | 101.05      | 98.38  | 92.19  | 104.60         | 101.83 | 99.60  | 103.02        | 107.10 | 100.26 |
| % RSD                    | 5.96        | 6.98   | 6.81   | 4.47           | 6.12   | 8.19   | 4.48          | 5.12   | 6.55   |

<sup>a</sup> OOS represents tablets out of specification of USP standard criteria.

The v-shaped depression became more pronounced at the later stage of tableting (60–100 min) as can be observed from the severely skewed distribution of the content uniformity data (Fig. 7(A-3)). The low amount of powder blend remaining and the hopper geometry (its funnel shape section with tapered end) led to rolling segregation, with the denser ordered units (lactose particles coated with  $\mu$ CMP) moving more rapidly downwards and the less dense MCC particles trailing behind at the upper portion of the

powder bed. Simultaneous collection of in-line blend uniformity data of the powder blend in the hopper, which was beyond the scope of this study, would be useful to demonstrate and confirm this occurrence of segregation in the hopper. Although changes in lactose and MCC concentrations were detected at the later stage of tableting, these changes were still within the scale of scrutiny observed in this study (Table 8). This could be traced to their much larger proportions in the blend/tablet matrix composition. As for

**Table 8**  
Summary of NIR prediction results (% potency) obtained from in-line and stratified sampling.

| Component             | Lactose |        |        | MCC    |        |        | MgSt   |        |        |
|-----------------------|---------|--------|--------|--------|--------|--------|--------|--------|--------|
|                       | 0–30    | 30–60  | 60–100 | 0–30   | 30–60  | 60–100 | 0–30   | 30–60  | 60–100 |
| <b>In-line NIR</b>    |         |        |        |        |        |        |        |        |        |
| Minimum               | 77.02   | 76.94  | 71.69  | 82.06  | 86.13  | 95.94  | 82.40  | 83.84  | 90.64  |
| Maximum               | 99.59   | 97.73  | 95.51  | 124.65 | 125.55 | 137.47 | 107.44 | 131.20 | 120.40 |
| Mean                  | 90.48   | 89.58  | 88.41  | 99.12  | 106.14 | 112.10 | 96.70  | 103.47 | 106.31 |
| % RSD                 | 3.29    | 3.17   | 2.75   | 5.88   | 5.56   | 4.47   | 4.08   | 4.49   | 2.99   |
| <b>Stratified NIR</b> |         |        |        |        |        |        |        |        |        |
| Minimum               | 93.66   | 91.12  | 83.06  | 94.89  | 96.47  | 94.35  | 89.37  | 92.42  | 89.58  |
| Maximum               | 105.06  | 103.25 | 99.44  | 112.13 | 115.45 | 115.99 | 105.68 | 109.58 | 110.74 |
| Mean                  | 97.65   | 96.79  | 95.75  | 103.99 | 103.34 | 105.47 | 98.26  | 101.32 | 101.35 |
| % RSD                 | 2.54    | 3.16   | 3.24   | 4.66   | 4.63   | 4.80   | 4.82   | 4.87   | 5.66   |

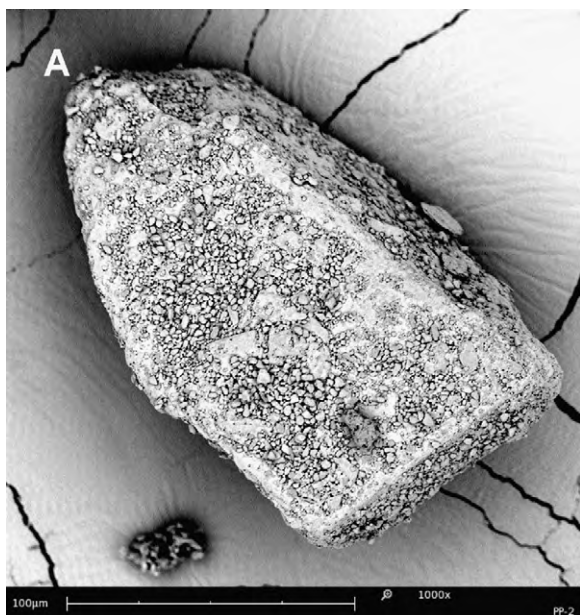


**Fig. 8.** Scanning electron micrograph of the ordered unit of coarse lactose particle coated with fine  $\mu$ CPM particles (1000 $\times$  magnification) obtained after high shear premixing.

MgSt, despite being present in a lower proportion, it showed uniform distribution due to its formation of a thin coat over the coarser excipients.

### 3.6. Analysis of tablets using stratified sampling

Results obtained with stratified sampling for  $\mu$ CPM are as shown in Table 7 and in the frequency distribution plots in Fig. 7 while the results for excipients are shown in Table 8. As can be seen from the results for  $\mu$ CPM content, both NIR and UV stratified sampling analysis of 30 tablets per time period showed that the whole batch met the standard specification for content uniformity and did not detect any content non-uniformity within the batch. This is because the probability of the tablet batch being passed as within the standard specification for content uniformity increases with decrease in sample size. Only exhaustive analysis of all the tablets produced would be able to reveal the potential content non-uniformity issues towards the later part of the tableting process. NIR in-line analysis showed significant number of tablets starting to fall outside the USP criteria when the batch reached the second half of the tableting cycle. NIR prediction results obtained for stratified sampled tablets did not reveal any aberrant distribution phenomenon for the excipients.

### 3.7. Continuous quality monitoring of the tableting process

US-FDA in its PAT guidance (FDA, 2004) encouraged pharmaceutical manufacturers to voluntarily develop and implement new technologies in pharmaceutical production and quality control for real time measurements of critical product and process parameters. PAT implies building quality into products through better understanding and control of the manufacturing process, rather than merely testing the quality of the end product. With the experimental set up discussed in this study, PAT goals of continuous quality monitoring of the process could be achieved successfully. As demonstrated, this in-line monitoring study may be used to identify out of specification (OOS) tablets in real time. This would not have been possible by following merely the pharmacopoeial requirement for sampling and testing of 30 tablets off-line.

Additionally, owing to the multi-sensing ability of NIR, it was possible to track the in-process distribution of excipients within the tablet matrix. Although the problem of non-uniform distribution of excipients was not observed in this study due to their relatively larger proportions in the tablet formulation, this analysis could be critical and of great value for formulations containing lower proportion excipients, such as super disintegrants or release modifiers, which are used in much smaller quantities and their uniform distribution is as critical as that of the drug for the performance of the dosage form.

## 4. Conclusion

This study demonstrated that the unique features of NIR for high speed sampling and rapid spectral acquisition enabled the quantification of individual tablet components with a high degree of accuracy during tableting. Due to inclusion of maximum possible variability encountered during tableting at the calibration stage, more sensitive prediction models were obtained which ultimately gave predictions of high accuracy. Furthermore, adequacy of the models for in-line quantification of individual tablet components was evident from the validation results. In-line analysis revealed the inadequacies associated with the commonly employed analysis of a smaller number of sampled tablets from the production batch. Sampling could not consistently identify the content uniformity problems and thus warranted the need for increasing the number of tablets to be analyzed before allowing the release of a tablet batch in certain cases. With the proposed setup, simultaneous quantification of drug and excipients in an efficient and non-destructive manner could be achieved. This is a step forward towards achieving the objectives laid out by the PAT guidelines.

## Acknowledgement

The authors wish to acknowledge research funding support from GEA-NUS PPRL fund (N-148-000-008-001) and would like to thank CAMO Inc. for the gratis supply of license for Unscrambler 9.8 and OLUP softwares.

## References

- Berman, J., Elinski, D.E., Gonzales, C.R., Hofer, J.D., Jimenez, P.J., Planchard, J.A., Tlachac, R.J., Vogel, P.F., 1997. Blend uniformity analysis: validation and in-process testing. Technical Report No. 25. PDA (Parenteral Drug Association). PDA J. Pharm. Sci. Technol. 51, S1–S99.
- Beebe, R., Pell, R.J., Seasholtz, M.B., 1998. Multivariate Calibration and Prediction. Chemometrics: A Practical Guide. John Wiley & Sons, New York, NY, pp. 280.
- Blanco, M., Coello, J., Iturriaga, H., Maspocho, S., Pezuela, C., 1997. Effect of data pre-processing methods in near-infrared diffuse reflectance spectroscopy for the determination of the active compound in a pharmaceutical component. Appl. Spectrosc. 51, 240–246.
- Blanco, M., Alcalá, M., 2006. Simultaneous quantitation of five active principles in a pharmaceutical preparation: development and validation of a near infrared spectroscopic method. Eur. J. Pharm. Sci. 27, 280–286.
- Blanco, M., Gozalez Bano, R., Bertran, E., 2002. Monitoring powder blending in pharmaceutical processes by use of near infrared spectroscopy. Talanta 56, 203–212.
- Blanco, M., Villarroya, I., 2002. NIR spectroscopy: a rapid-response analytical tool. TrAC - Trends Anal. Chem. 21, 240–250.
- Cogdill, R.P., Anderson, C.A., Delgado-Lopez, M., Molseed, D., Chisholm, R., Bolton, R., Herkert, T., Afnan, A.M., Drennen III, J.K., 2005. Process analytical technology case study part I: feasibility studies for quantitative near-infrared method development. AAPS Pharm. Sci. Tech. 6, E262–E272.
- Colon, N.J., Peroza, C., Caraballo, W., Conde, C., Li, T., Morris, K.R., Romanach, R.J., 2005. On line non-destructive determination of drug content in moving tablets using near infrared spectroscopy. J. Proc. Anal. Tech. 2, 8–15.
- Cournoyer, A., Simard, J.S., Cartilier, L., Abatzoglou, N., 2008. Quality control of multi-component, intact pharmaceutical tablets with three different near-infrared apparatuses. Pharm. Dev. Technol. 13, 333–343.
- El-Hagrasy, A.S., Drennen III, J.K., 2006. A process analytical technology approach to near-infrared process control of pharmaceutical powder blending. Part III: quantitative near-infrared calibration for prediction of blend homogeneity and characterization of powder mixing kinetics. J. Pharm. Sci. 95, 422–434.

- Esbensen, K.H., 2004. *Multivariate Data Analysis-In Practice*. CAMO Process AS, Oslo, Norway.
- Gottfries, J., Depui, H., Fransson, M., Jongeneelen, M., Josefson, M., Langkilde, F.W., Witte, D.T., 1996. Vibrational spectrometry for the assessment of active substance in metoprolol tablets: a comparison between transmission and diffuse reflectance near-infrared spectrometry. *J. Pharm. Biomed. Anal.* 14, 1495–1503.
- Honigs, D.E., 1992. Three constant themes in NIR analysis. In: Hildrum, K.I., Isaksson, T., Naes, T., Tandberg, A. (Eds.), *Near Infra-Red Spectroscopy: Bridging the Gap between Data Analysis and NIR Applications*. Ellis Harwood Ltd., Sussex, pp. 109–118.
- ICH, 2005. *Validation of Analytical Procedures: Text and Methodology Q2 (R1)*.
- Li, T., Donner, A.D., Choi, C.Y., Frunzi, G.P., Morris, K.R., 2003. A statistical support for using spectroscopic methods to validate the content uniformity of solid dosage forms. *J. Pharm. Sci.* 92, 1526–1530.
- Liew, C.V., Karande, A.D., Heng, P.W.S., 2010. In-line quantification of drug and excipients in cohesive powder blends by near infrared spectroscopy. *Int. J. Pharm.* 386, 138–148.
- Luybaert, J., Massart, D.L., Vander Heyden, Y., 2007. Near-infrared spectroscopy applications in pharmaceutical analysis. *Talanta* 72, 865–883.
- Marten, H., Naes, T., 1989. *Multivariate Calibration*. John Wiley & Sons, New York, NY.
- Meza, C.P., Santos, M.A., Romañach, R.J., 2006. Quantitation of drug content in a low dosage formulation by transmission near infrared spectroscopy. *AAPS Pharm. Sci. Tech.*, 7.
- Olinger, J.M., Griffiths, P.R., 1993a. Effects of sample dilution and particle size/morphology on diffuse reflection spectra of carbohydrate systems in the near- and mid-infrared. I. Single analytes. *Appl. Spectrosc.* 47, 687–694.
- Olinger, J.M., Griffiths, P.R., 1993b. Effects of sample dilution and particle size/morphology on diffuse reflection spectra of carbohydrate systems in the near- and mid-infrared. II. Durum wheat. *Appl. Spectrosc.* 47, 695–701.
- Reich, G., 2005. Near-infrared spectroscopy and imaging: basic principles and pharmaceutical applications. *Adv. Drug Deliv. Rev.* 57, 1109–1143.
- Roggo, Y., Chalus, P., Maurer, L., Lema-Martinez, C., Edmond, A., Jent, N., 2007. A review of near infrared spectroscopy and chemometrics in pharmaceutical technologies. *J. Pharm. Biomed. Anal.* 44, 683–700.
- Romanach, R.J., Santos, M.A., 2003. Content uniformity testing with near infrared spectroscopy. *Am. Pharm. Rev.* 6, 62–67.
- Sallam, E., Orr, N., 1985. Content uniformity of ethinyldestradiol tablets 10 µg: effect of variations in processing on the homogeneity after dry mixing and after tableting. *Drug Dev. Ind. Pharm.* 11, 607–633.
- Scheiwe, M.W., Schilling, D., Aebi, P., 1999. Near infrared spectroscopy analysis of intact pharmaceutical diclofenac coated tablets in transmission. *Pharmazeutische Industrie* 61, 179–183.
- Thosar, S.S., Forbess, R.A., Ebube, N.K., Chen, Y., Rubinovitz, R.L., Kemper, M.S., Reier, G.E., Wheatley, T.A., Shukla, A.J., 2001. A comparison of reflectance and transmittance near-infrared spectroscopic techniques in determining drug content in intact tablets. *Pharm. Dev. Technol.* 6, 19–29.
- Uniformity of Dosage Units, 2009. *United States Pharmacopeia*, pp. 382–383.
- U.S. Food and Drug Administration, 2004. *Guidance for industry, PAT-A framework for innovative pharmaceutical development, manufacturing and quality assurance*.
- Westad, F., Bystrom, M., Martens, H., 1999. Modified Jack-knifing in multivariate regression for variable selection and model stability, NIR-99. In: *Proceedings, International Symposium on NIR Spectroscopy, Verona*.